Fuel 93 (2012) 658–669

Contents lists available at SciVerse ScienceDirect

Fuel

journal homepage: www.elsevier.com/locate/fuel

PC-SAFT characterization of crude oils and modeling of asphaltene phase behavior

Sai R. Panuganti [a], Francisco M. Vargas [b,*], Doris L. Gonzalez [c], Anjushri S. Kurup [a], Walter G. Chapman [a]

[a] Department of Chemical and Biomolecular Engineering, Rice University, Houston, TX 77005, USA
[b] Department of Chemical Engineering, Petroleum Institute, Abu Dhabi, United Arab Emirates
[c] Data Quality Group, Schlumberger, Houston, TX 77056, USA

ARTICLE INFO

Article history:
Received 11 February 2011
Received in revised form 9 September 2011
Accepted 13 September 2011
Available online 8 October 2011

Keywords:
Characterize
Crude oil
Bubble pressure
Asphaltene onset pressure
Phase plot

ABSTRACT

Asphaltenes are the heaviest and most polarizable components of crude oil. The phase behavior of these polydisperse components is important in both the upstream and downstream processing of crude oil because of their potential to precipitate, deposit and plug pipelines and production equipment. Predicting flow assurance issues caused by asphaltenes requires the ability to model the phase behavior of asphaltenes as a function of temperature, pressure, and composition. In this work we present a detailed procedure to characterize crude oil and plot asphaltene phase envelope, using the Perturbed Chain form of the Statistical Associating Fluid Theory (PC-SAFT). This work also demonstrates that the proposed procedure can model the asphaltene thermodynamic phase behavior better than using a cubic equation of state typically used in the industry, even with compositional data as low as C_9+.

The results obtained with the proposed characterization method show a remarkable matching with the experimental data points for both the bubble point and asphaltene precipitation onset curves. A wide range of temperatures, pressures and gas injection percentages have been tested. In this work, the concept of lower asphaltene onset pressure is also clarified and a new representation of asphaltene phase plot is presented. The results obtained in this work are very promising in providing better tools to model asphaltene phase behavior.

1. Introduction

Asphaltenes are the heaviest and most polarizable fraction of crude oil [1]. They are operationally defined in terms of their solubility as the components of crude oil that are completely miscible in aromatic solvents, such as benzene, toluene or xylenes, but insoluble in light paraffinic solvents, such as *n*-pentane or *n*-heptane at ambient conditions [2,3]. Asphaltenes are of particular interest to the petroleum industry because of their deposition tendencies in production equipment that cause considerable production costs [4]. In addition, precipitated asphaltenes impart high viscosity to crude oils, negatively impacting production [5].

Among the flow assurance problems in the Middle East, asphaltene deposition in production wells are one of the major concerns [6]. Hence, as a starting step prediction of asphaltene precipitation is important towards understanding deposition problems [7]. Tendency of asphaltene to precipitate can be best understood from its phase behavior with respect to pressure, temperature and composition of the system. However, a typical crude oil has numerous components and computing the phase behavior by considering these components individually becomes computationally expensive. On the contrary, characterizing the oil as a mixture of well defined fractions that represent blends of similar components in oil, instead of handling the components individually can aid in reducing the computational cost significantly.

One of the earliest studies on crude oil characterization dates back to 1978 by Katz and Firoozabadi [8] where boiling point temperatures were used for separating the carbon number fraction. The cut points were determined from the boiling points of *n*-paraffins. The resulting densities are for paraffinic oils and therefore very low [9]. Later work (1983) on characterizing crude oils by Whitson [10] subdivided crude oils into different single carbon number (SCN). This has been the most widely applied procedure for upstream applications. It is based on average boiling point of each SCN cut and uses correlations from Riazi and Daubert published in 1980 [11]. Typical representation of Whitson characterization for a Middle East light crude oil (crude A) is presented in Table 1. In this case the plus fraction component (C_{36}+) represents all higher molecular weight components above C_{36}.

The reservoir fluid which is monophasic is usually flashed from reservoir pressure and temperature to ambient conditions to yield residual liquid/stock tank oil (STO) and evolved gas phase/flashed gas which are then analyzed for composition using gas chromatography. The live oil composition is computed using gas-to-oil ratio (GOR).

* Corresponding author. Tel.: +971 2 607 5456.
E-mail addresses: sai@rice.edu (S.R. Panuganti), fvargas@pi.ac.ae (F.M. Vargas), DGonzalez21@slb.com (D.L. Gonzalez), anjushri.s.kurup@rice.edu (A.S. Kurup), wgchap@rice.edu (W.G. Chapman).

0016-2361/$ - see front matter © 2011 Elsevier Ltd. All rights reserved.
doi:10.1016/j.fuel.2011.09.028

Table 1
Typical representation of Whitson characterization for a Middle East light crude oil (crude A).

Component	MW (g/mol)	Density (g/cc)	Flashed gas		STO		Reservoir fluid (GOR-787 scf/stb)	
			wt.%	mol%	wt.%	mol%	wt.%	mol%
N_2	28.04	0.809	0.270	0.280	0	0	0.047	0.163
CO_2	44.01	0.817	5.058	3.340	0	0	0.874	1.944
H_2S	34.08	0.786	0	0	0	0	0	0
C_1	16.04	0.300	31.858	57.716	0	0	5.503	33.600
C_2	30.07	0.356	13.431	12.981	0.044	0.279	2.356	7.557
C_3	44.10	0.508	17.571	11.581	0.296	1.294	3.280	6.742
iC_4	58.12	0.567	5.280	2.640	0.251	0.835	1.120	1.884
nC_4	58.12	0.586	11.74	5.871	0.923	3.066	2.792	4.695
iC_5	72.15	0.625	4.593	1.850	0.999	2.673	1.620	2.195
nC_5	72.15	0.631	5.139	2.070	1.589	4.250	2.202	2.984
C_6	84.00	0.690	3.497	1.210	3.593	8.254	3.576	4.162
Mcyclo-C_5	84.16	0.749	0	0	0.447	1.024	0.369	0.429
Benzene	78.11	0.876	0	0	0.143	0.354	0.119	0.148
Cyclo-C_6	84.16	0.779	0	0	0.322	0.739	0.267	0.310
C_7	96.00	0.727	1.222	0.370	3.604	7.245	3.193	3.251
Mcyclo-C_6	98.19	0.770	0	0	0.619	1.217	0.512	0.510
Toluene	92.14	0.867	0	0	0.702	1.471	0.581	0.616
C_8	107.00	0.749	0.258	0.070	3.805	6.862	3.192	2.916
C_2-benzene	106.17	0.866	0	0	0.224	0.407	0.185	0.171
m&p Xylene	106.17	0.860	0	0	0.644	1.171	0.533	0.491
o Xylene	106.17	0.860	0	0	0.038	0.069	0.032	0.029
C_9	121	0.768	0.083	0.020	3.936	6.277	3.270	2.642
C_{10}	134	0.782	0	0	4.605	6.632	3.809	2.779
C_{11}	147	0.793	0	0	3.787	4.971	3.132	2.083
C_{12}	161	0.804	0	0	3.241	3.885	2.682	1.628
C_{13}	175	0.815	0	0	3.096	3.414	2.561	1.431
C_{14}	190	0.826	0	0	2.929	2.975	2.423	1.247
C_{15}	206	0.836	0	0	2.83	2.651	2.341	1.111
C_{16}	222	0.843	0	0	2.437	2.150	2.046	0.901
C_{17}	237	0.851	0	0	2.356	1.918	1.949	0.804
C_{18}	251	0.856	0	0	2.128	1.636	1.761	0.686
C_{19}	263	0.861	0	0	2.231	1.637	1.845	0.686
C_{20}	275	0.866	0	0	2.193	1.539	1.814	0.645
C_{21}	291	0.871	0	0	1.900	1.260	1.572	0.528
C_{22}	300	0.876	0	0	1.805	1.161	1.493	0.486
C_{23}	312	0.881	0	0	1.628	1.007	1.346	0.422
C_{24}	324	0.885	0	0	1.512	0.900	1.250	0.377
C_{25}	337	0.888	0	0	1.417	0.811	1.172	0.340
C_{26}	349	0.892	0	0	1.377	0.761	1.139	0.319
C_{27}	360	0.896	0	0	1.269	0.680	1.050	0.285
C_{28}	372	0.899	0	0	1.280	0.664	1.059	0.278
C_{29}	382	0.902	0	0	1.079	0.545	0.893	0.228
C_{30}	394	0.903	0	0	1.031	0.505	0.853	0.212
C_{31}	404	0.907	0	0	0.937	0.448	0.775	0.188
C_{32}	415	0.910	0	0	0.883	0.411	0.731	0.172
C_{33}	426	0.913	0	0	0.803	0.364	0.664	0.152
C_{34}	437	0.916	0	0	0.694	0.307	0.574	0.129
C_{35}	445	0.919	0	0	0.666	0.289	0.551	0.121
C_{36}+	594	0.941	0	0	27.673	8.991	22.893	3.767

Whitson's method provides a set of physical properties such as the average boiling point, specific gravity and molecular weight for petroleum fractions containing C_6 and higher based on the analysis of the physical properties of liquid hydrocarbons and condensates. However, this characterization method leads to significant errors when applied to heavier components as shown by Tarek in 1989 [12] and hence the oil modeled by this method does not provide a close representation of the entire crude oil.

Whitson's method was followed by the paraffins–naphthenes–aromatics method to characterize crude liquid phase and is based on the refractive index (RI) data. The method was proposed when correlations of Riazi–Daubert used by Whitson were unable to represent the entire crude oil. In 1996 Riazi [13,14] provided equations for calculating boiling point, density, RI, critical temperature, pressure and density, acentric factor, surface tension and solubility parameter of SCN hydrocarbon groups for C_6–C_{50} existing in crude oils and hydrocarbon-plus fractions. Leelavanichkul in 2004 [15] used the paraffins–naphthenes–aromatics technique to characterize different hydrocarbon fluids in a solid–liquid model designed to determine wax and asphaltene precipitation onsets. However, the solubility parameter for C_{50} fraction was too low to represent the heaviest fractions in a crude oil. Also the maximum refractive index does not reach the expected 1.7 value that has been estimated for asphaltenes in different investigations [16].

The above mentioned characterization procedures employ a cubic equation of state (cubic EoS). Along with the deficiencies in characterization procedures, the cubic EoS predictions are poor for molecules of different sizes and the EoS parameters for asphaltenes are not well defined because the asphaltene critical properties and acentric factor are not well known [17]. A more recent and promising equation of state is the SAFT based EoS [18,19]. This equation of state based on statistical mechanics can accurately model mixtures of different molecular sizes. But a lack of definite characterization procedure hindered its industrial use [20]. In this work, a detailed characterization procedure using a SAFT based EoS is outlined which will enable the easy usage of this EoS for modeling the phase behavior of asphaltenes. The PC-SAFT modeled asphaltene phase behavior is compared to that of a cubic EoS.

The phase plot is extended further to include the lower onset of asphaltene and the amount of asphaltene precipitated.

The characterization procedure is an extension of work reported by Ting in 2003 [21]. This work uses the perturbed chain version of SAFT (PC-SAFT), developed by Gross and Sadowski [22]. It has been demonstrated that PC-SAFT can accurately predict the phase behavior of high molecular weight compounds [23] similar to the large asphaltene molecules, and PC-SAFT is also available in commercial simulators such as Multiflash of InfoChem and VLXE of VLXE Aps.

2. Characterization methodology

Carbon content in a crude oil is almost entirely present as saturates and unsaturates [24]. This identity is made use of in the proposed characterization procedure to model crude oil with a small number of components. The characterized system consists of gas phase and liquid phase which are then recombined according to GOR to simulate live oil.

2.1. Gas components

The gas phase is characterized to consist of seven components: N_2, CO_2, H_2S, methane, ethane, propane and heavy gas pseudo-component that represents a mixture of hydrocarbons heavier than propane. It has been observed that the light components in oil affect both the bubble pressure and asphaltene onset pressure (AOP) significantly [25]. Hence in this work, the lightest fractions of oil will be considered individually which should result in better prediction of asphaltene onset pressures. Also, the injected gas typically used for enhanced oil recovery (EOR) purposes is generally rich in lighter hydrocarbons and hence the methodology proposed in this work will enable good predictions even for these gas injection situations and will be demonstrated in the results and discussion section.

2.2. Liquid components

The liquid fraction characterization into saturates, aromatics + resins (A + R) and asphaltenes is based on the STO composition and the saturates, aromatics, resins and asphaltenes (SARA) analysis.

2.2.1. Saturates pseudo-component

The saturates pseudo-component represents normal alkanes (*n*-paraffins), branched alkanes (iso-paraffins) and cyclo-alkanes (naphthenes) present in the stock tank oil. They are defined as the fraction of STO soluble at room temperature in *n*-heptane.

2.2.2. Aromatics + resins pseudo-component

In the SARA analysis of STO, aromatics are determined by adsorption chromatography, typically from silica or silica/alumina and resins from clay packed column adsorption. The total amount of aromatics and resins fraction distribute along the liquid phase, proportionally with the saturates fraction as dictated by the SARA analysis. The aromatics and resin fractions are combined into a single lumped pseudo-component defined in terms of the degree of aroma ticity (γ). This parameter determines the tendency of the aromatics + resins pseudo-component to behave as a poly-nuclear-aromatic (PNA) ($\gamma = 1$) or as a benzene derivative component ($\gamma = 0$) [26]. In the characterization procedure of different crude oils, the aromaticity value is adjusted to meet the saturation pressure and density of the crude oil. The aromaticity value is thus typically adjusted between 0 and 1.

2.2.3. Asphaltenes

Asphaltenes, as mentioned before, are defined by their solubility. Asphaltenes exist as pre-aggregated molecules even in good solvents such as toluene [27,28]. Hence, in this work, the average molecular weight (MW) for such nano-sized pre-aggregated asphaltene is considered as 1700 g/mol [21,25,29]. Variations in asphaltene parameters have negligible effect on saturation pressures and density of crude oil, because asphaltenes have very low vapor pressure and are generally present in small amounts in crude oil.

2.3. The following is the characterization procedure

2.3.1. Characterization of flashed gas

The flashed gas is modeled as a mixture of seven compounds: N_2, CO_2, H_2S, C_1 (methane), C_2 (ethane), C_3 (propane) and heavy gas (lumped C_4+ components). Benzene, toluene and xylene are not added in the compositional analysis of flashed gas since they are present in very small quantities and hence do not significantly impact the predictions. Moreover, these components belong to the aromatics class and cannot be lumped into the heavy gas fraction containing saturates. Considering these components separately increases the number of components in the modeled gas increasing the computational time without significant advantage. Table 2 represents the characterized gas phase of crude oil A.

2.3.2. Characterization of STO

While characterizing the liquid phase, the mole percentage of compositional data is converted to weight percentage to match with the SARA data. From a typical crude oil composition data, all the components that are C_9 and above are lumped into C_9+ fraction with an average MW. As discussed before, the asphaltene MW is presumed as 1700 g/mol. The C_9+ MW of the saturates and aromatics + resins pseudo components are assumed such that the STO MW and C_9+ average MW are matched. Amounts of C_9+ saturates, A + R and asphaltenes pseudo-components are inputted such that the total weight percentages of saturates, aromatics plus resins and asphaltene match the content reported in SARA. Table 3 shows the characterized STO of crude oil A.

Gas-to-oil ratio which is operationally specified in scf/stb or m^3/m^3 is converted in terms of (moles of gas)/(moles of liquid). With a basis of total moles of live oil as 100, individual moles contribution from components towards flashed gas and STO are calculated and hence the mole percentage of all components in live oil. Table 4 is the representation of characterized live oil of crude A with its components.

2.3.3. Parameters estimation

It is established by the works of Hirasaki and Buckley that it is not polarity but polarizability that dominates asphaltene phase behavior [16,30]. Because of this, the association term in SAFT is not used in this asphaltene modeling work and the PC-SAFT EoS requires just three parameters for each non-associating component. These parameters are the temperature-independent diameter of each molecular segment (σ), the number of segments per molecule (m), and the segment–segment dispersion energy (ε/k).

PC-SAFT parameters (m, σ and ε/k) for N_2 to C_3 are pre defined through the works of Gross and Gonzalez separately [22,26] and are summarized in Table 5. PC-SAFT parameters for heavy gas/saturates, aromatics + resins are also well established through the work of Gonzalez and Ting [26,31]. The correlations are shown in Fig. 1 and summarized in Table 6. The parameter of aromaticity (γ) used in these correlations determines the aromatics + resins pseudo-component tendency to behave as a poly-nuclear-aromatic (PNA) ($\gamma = 1$) or as a benzene derivative component ($\gamma = 0$).

Table 2
Characterized gas phase for crude A.

Flashed gas			Modeled gas		
Component	MW	mol%	Component	MW	mol%
N_2	28.04	0.28	N_2	28.04	0.29
CO_2	44.01	3.34	CO_2	44.01	3.59
H_2S	34.08	0.00	H_2S	34.08	0.00
C_1	16.04	57.72	C_1	16.04	59.79
C_2	30.07	12.98	C_2	30.07	13.00
C_3	44.10	11.58	C_3	44.10	10.36
iC_4	58.12	2.64	Heavy gas	65.4	14.08
nC_4	58.12	5.87			
iC_5	72.15	1.85			
nC_5	72.15	2.07			
C_6	84.00	1.21			
Mcyclo-C_5	84.16	0.00			
Benzene	78.11	0.00			
Cyclo-C_6	84.16	0.00			
C_7	96.00	0.37			
Mcyclo-C_6	98.19	0.00			
Toluene	92.14	0.00			
C_8	107.00	0.07			
C_2-benzene	106.17	0.00			
m&p Xylene	106.17	0.00			
o Xylene	106.17	0.00			
C_9	121	0.02			

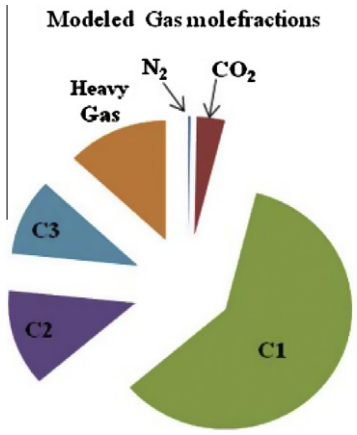

Table 3
Characterized stock tank oil for crude A.

Component	MW (g/mol)	Basis 100 g of STO (mass %)	Saturates		Aromatics + resins		Asphaltenes			
			Mass (g)	mol%	Mass (g)	mol%	Component	MW	Mass	mole
N_2	28.04	0	0	0	0	0	Asphaltenes	1700	2.8	0.0016
CO_2	44.01	0	0	0	0	0				
H_2S	34.08	0	0	0	0	0				
C_1	16.04	0	0	0	0	0				
C_2	30.07	0.04	0.04	0.37	0	0				
C_3	44.10	0.30	0.30	1.70	0	0				
iC_4	58.12	0.25	0.25	1.10	0	0				
nC_4	58.12	0.92	0.92	4.03	0	0				
iC_5	72.15	1.00	1.00	3.52	0	0				
nC_5	72.15	1.59	1.59	5.60	0	0				
C_6	84.00	3.59	3.59	10.87	0	0				
Mcyclo-C_5	84.16	0.45	0.45	1.35	0	0				
Benzene	78.11	0.14	0	0	0.14	1.50				
Cyclo-C_6	84.16	0.32	0.32	0.97	0	0				
C_7	96.00	3.60	3.60	9.54	0	0				
Mcyclo-C_6	98.19	0.62	0.62	1.60	0	0				
Toluene	92.14	0.70	0	0	0.70	6.20				
C_8	107	3.80	3.80	9.04	0	0				
C_2-benzene	106.00	0.22	0	0	0.22	1.72				
m&p Xylene	106.17	0.64	0	0	0.64	4.94				
o Xylene	106.17	0.04	0	0	0.04	0.29				
C_9+	268.4	81.72	49.5	50.31	29.42	85.36				
			C_9 + Sat MW 250	C_9 + Sat MW 280.6						

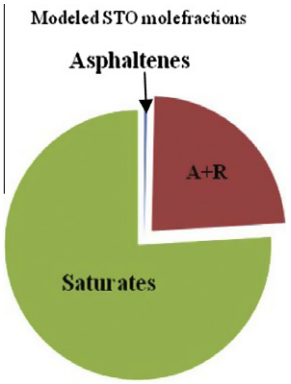

Initially PC-SAFT parameters for asphaltenes are set as: $m = 33$, $\sigma = 4.3$ and $\varepsilon/k = 400$ [32]. The constant set of PC-SAFT temperature independent binary interaction parameters (K_{ij}) are well established (Table 7) by adjusting binary vapor–liquid equilibrium for the combination of pure components. The references in Table 7 indicate the data used to establish interaction parameters. With all the initial parameters set, density of crude oil is calculated using PC-SAFT. Accordingly, aromaticity is adjusted to match the given density and bubble pressure simultaneously. Only after the aromaticity is set, PC-SAFT parameters of asphaltene are adjusted to match the experimentally observed onset pressures.

The asphaltene onset pressure (AOP) is the cloud point at a fixed temperature for which the crude oil will split up into 2 liquid phases of asphaltene rich and lean phases [65]. Such measurements can involve depressurization of live oil or titration of dead oil with a precipitant. In order to match a given set of asphaltene onset pressure, asphaltene PC-SAFT parameters can be varied according to the selection rules proposed by Ting [31]. It has been observed that experimental errors while calculating AOP using the near infrared technique (NIR) vary between ±250 psia.

Table 8 summarizes the adjusted parameters.

3. Results and discussion

In the current study three crude oils (A, B and C) are considered. The properties of the crudes are listed in Table 9. Crude oils A, B

Table 4
Characterized live oil of crude A as a combination of nine components.

Component	MW (g/mol)	Contribution from gas (moles)	Contribution from STO (moles)	Moles in live oil Basis 100	Characterized live oil
N_2	28.04	0.163	0	0.163	
CO_2	44.01	1.944	0	1.944	
C_1	16.04	33.600	0	33.600	
C_2	30.07	7.557	0	7.557	
C_3	44.10	6.742	0	6.742	
Heavy gas	65.49	8.198	0	8.198	
Saturates	167.68	0	31.743	31.743	
Aromatics + resins	253.79	0	9.907	9.907	
Asphaltenes	1700	0	0.133	0.133	

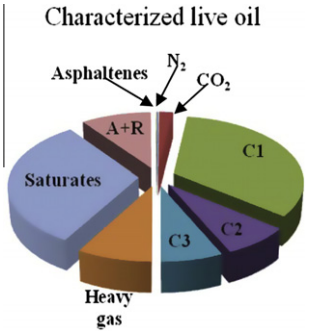

Table 5
PC-SAFT parameters for light components in crude oil [22].

Component	m	σ (A)	ε/k (K)
N_2	1.206	3.313	90.96
CO_2	2.073	2.785	169.21
H_2S	1.6517	3.0737	227.34
C_1	1.000	3.704	150.03
C_2	1.607	3.520	191.42
C_3	2.002	3.618	208.11

and C are similar in nature, given their location. The PC-SAFT characterized crude oils A, B and C along with the parameters are reported in Tables 10–12 respectively. It can be noted that the asphaltene PC-SAFT parameters differ between the oils because asphaltenes of different crude oils behave differently [66].

3.1. PC-SAFT parameter estimation

The previous PC-SAFT characterization for crude oil lacked a complete experimental data [25]. Here, we report a new characterization procedure when minimum data is available. Ethane (C_2) and propane (C_3) constitute almost 20% of flashed gas (from Table 2) and injected gas (N_2-0.4%, CO_2-3.9%, C_1-71.4%, C_2-12%, C_3-7.2%, heavy gas-5.1%; all reported in mole percentage). Previously ethane and propane were lumped along with heavy gas even though these gases had significant concentration. Now they are considered separately giving more flexibility in the binary interaction parameters and hence a better parameter estimation. Previously all single carbon number (SCN) fractions even if present as high as C_{35}+, were individually split into saturates, aromatics + resins governed by SARA data with asphaltenes appearing only in the heaviest fraction of SCN [67]. Then they were regrouped into saturates, aromatics and resins components. Now, SCN after xylenes are lumped into one fraction and then split according to SARA analysis thereby reducing the computation time and the requirement to define SCN beyond C_9. Comparison between old and new PC-SAFT characterization results for crude A is represented using Fig. 2 where the discontinuous line represents the predictions made using the old PC-SAFT characterization method and the continuous line represents the predictions made with the new characterization procedure.

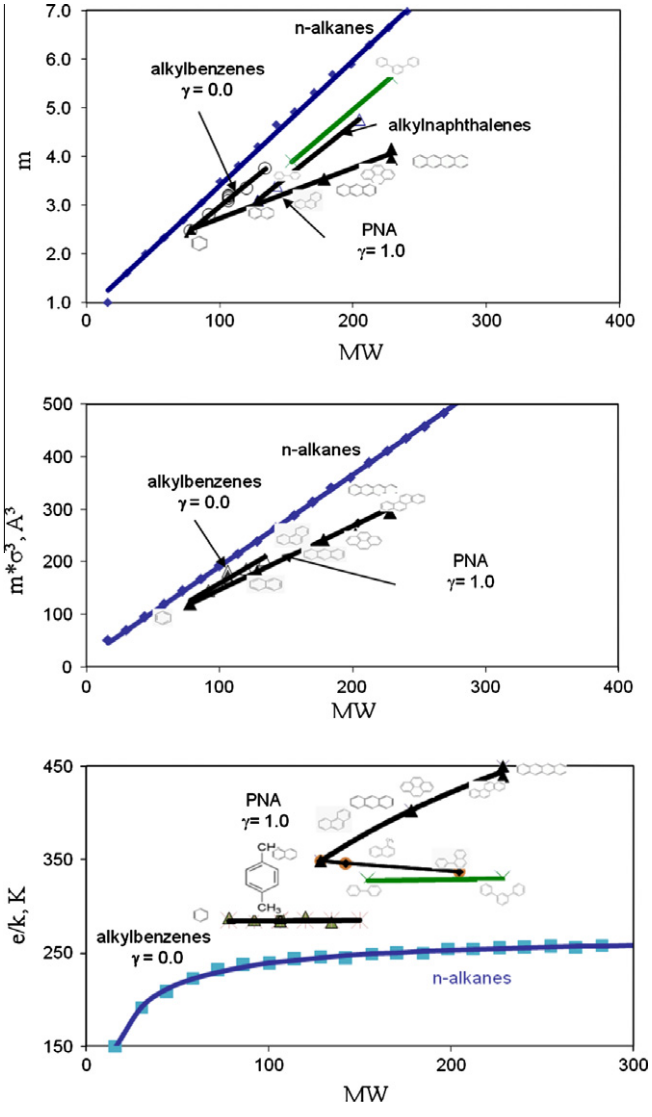

Fig. 1. Variation of PC-SAFT parameters for different homologous series [26].

Table 6
PC-SAFT correlations observed in Fig. 1 can be summarized as below [26].

Correlation for saturates	Aromatics + resins pseudo component (γ is aromaticity)parameter = $(1-\gamma)$ (benzene derivatives correlation) + γ(PNA correlation)
$m = (0.0257 * \mathrm{MW}) + 0.8444$	$m = (1-\gamma)(0.0223 * \mathrm{MW} + 0.751) + \gamma(0.0101 * \mathrm{MW} + 1.7296)$
$\sigma(A) = 4.047 - \frac{4.8013 * Ln(\mathrm{MW})}{\mathrm{MW}}$	$\sigma(A) = (1-\gamma)\left(4.1377 - \frac{38.1483}{\mathrm{MW}}\right) + \gamma\left(4.6169 - \frac{93.98}{MW}\right)$
$Ln(\varepsilon/k) = 5.5769 - \frac{9.523}{\mathrm{MW}}$, K	$\varepsilon/k = (1-\gamma)(0.00436 * \mathrm{MW} + 283.93) + \gamma\left(508 - \frac{234100}{(\mathrm{MW})^{1.5}}\right)$, K

Table 7
PC-SAFT temperature independent binary interaction parameters (K_{ij}) for a crude oil.

Component	N_2	CO_2	H_2S	C_1	C_2	C_3	Heavy gas	Saturates	Aromatics + resins	Asphaltenes
N_2	0	0 [33]	0.09 [34]	0.03 [35]	0.04 [36]	0.06	0.075 [37]	0.14 [38]	0.158 [39]	0.16
CO_2		0	0.0678 [40]	0.05 [41]	0.097 [42]	0.1 [43]	0.12 [44]	0.13 [45]	0.1 [46]	0.1 [26]
H_2S			0	0.062 [47]	0.058 [48]	0.053 [49]	0.07 [50]	0.09 [51]	0.015 [52]	0.015
C_1				0	0 [53]	0 [54]	0.03 [55]	0.03 [56]	0.029 [57]	0.07
C_2					0	0 [58]	0.02	0.012 [59]	0.025 [60]	0.06
C_3						0	0.015 [61]	0.01	0.01 [62]	0.01
Heavy gas							0	0.005 [63]	0.012 [64]	0.01 [26]
Saturates								0	0.007 [62]	−0.004
Aromatics + resins									0	0 [26]
Asphaltenes										0

Table 8
Adjusted parameters.

Parameter	Purpose	Remarks
Aromaticity	To match density and bubble pressure	Density and bubble pressure are matched simultaneously
The three PC-SAFT asphaltene parameters (m, σ and ε/k)	To match asphaltene onset pressure	To be estimated only after aromaticity is set

Table 9
Properties of crude oils A, B and C.

	Crude A	Crude B	Crude C
GOR (scf/stb)	787	798	852
MW of reservoir fluid (g/mol)	97.750	96.15	92.78
MW of flashed gas (g/mol)	29.064	28.54	30.24
MW of STO (g/mol)	193	191	182
STO density (g/cc)	0.823	0.823	0.817
Saturates (wt%)	66.26	75.56	73.42
Aromatics (wt%)	25.59	20.08	19.32
Resins (wt%)	5.35	4.13	7.05
Asphaltene (wt%)	2.8	0.21	0.17

3.2. Comparison of cubic and PC-SAFT EoS

Despite their poor prediction of asphaltene properties, cubic EoS [68] are widely used in the oil industry due to the simplicity of models. However, it is seen that the parameters fit using a cubic equation of state for a particular data set fails to predict another situation for the same well. This is demonstrated in the present work. Employing the well optimized characterization procedure [20] available in PVT-Sim (Version 18) from Calsep, crude B is characterized and parameters are fit to the saturation pressures and asphaltene onset pressures for various temperatures for this oil with 5% gas injection (mol%) using an SRK with Peneloux correction (discontinuous line in Fig. 3B). The same parameters are then used to predict the saturation pressure and temperature dependence of asphaltene onset pressure for different amounts of gas injected. Crude B is also characterized using the proposed PC-SAFT characterization method. Similar to the cubic EoS, the PC-SAFT parameters are obtained by estimating the EoS predictions to experimental data of saturation and onset pressures for oil with 5% gas injection (mol%) (continuous line in Fig. 3B). The same set of parameters was then used to predict the phase behavior for different injected gas amounts. PC-SAFT and the cubic EoS characterization are plotted together for each injected gas amounts and the predictions made by the EoS are compared in Fig. 3A, C and D. We can see that only PC-SAFT does a very good job in predicting the phase behavior of asphaltenes for various gas injection amounts.

Table 10
PC-SAFT characterized crude A.

Component	MW (g/mol)	mol%	PC-SAFT parameters		
			m	σ (A)	ε/k (K)
N_2	28.04	0.163	1.206	3.313	90.96
CO_2	44.01	1.944	2.073	2.785	169.21
C_1	16.04	33.600	1.000	3.704	150.03
C_2	30.07	7.557	1.607	3.520	191.42
C_3	44.10	6.742	2.002	3.618	208.11
Heavy gas	65.49	8.198	2.530	3.740	228.51
Saturates	167.68	31.743	5.150	3.900	249.69
Aromatics + resins (γ = 0.0)	253.79	9.907	6.410	3.990	285.00
Asphaltenes	1700.00	0.133	32.998	4.203	353.50

Table 11
PC-SAFT characterized crude B.

Component	MW (g/mol)	mol%	PC-SAFT parameters		
			m	σ (A)	ε/k (K)
N_2	28.04	0.169	1.206	3.313	90.96
CO_2	44.01	2.096	2.073	2.785	169.21
C_1	16.04	34.865	1.000	3.704	150.03
C_2	30.07	7.578	1.607	3.520	191.42
C_3	44.10	6.042	2.002	3.618	208.11
Heavy gas	67.12	7.560	2.570	3.750	229.32
Saturates	176.08	34.152	5.370	3.910	250.36
Aromatics + resins (γ = 0.05)	256.14	7.527	6.360	4.000	293.30
Asphaltenes	1700.00	0.010	37.220	4.493	413.54

Table 12
PC-SAFT characterized crude C.

Component	MW (g/mol)	mol%	PC-SAFT parameters		
			m	σ (A)	ε/k (K)
N_2	28.04	0.147	1.206	3.313	90.96
CO_2	44.01	1.716	2.073	2.785	169.21
C_1	16.04	32.558	1.000	3.704	150.03
C_2	30.07	7.889	1.607	3.520	191.42
C_3	44.10	7.287	2.002	3.618	208.11
Heavy gas	66.36	9.310	2.550	3.740	228.95
Saturates	169.17	32.630	5.190	3.900	249.81
Aromatics + resins (γ = 0.22)	234.78	8.456	5.570	4.030	319.70
Asphaltenes	1700.00	0.007	35.750	4.484	413.42

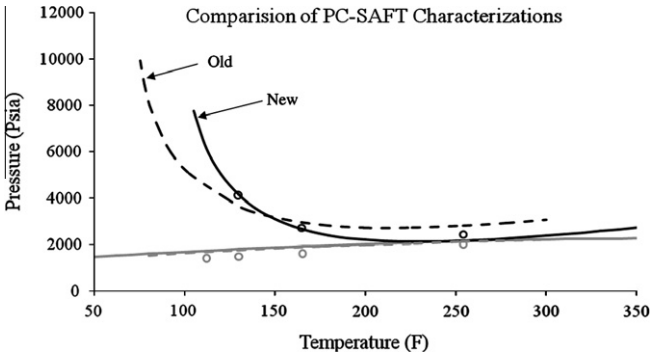

Fig. 2. Comparison of old and new PC-SAFT characterization procedures using crude A (black line: AOP; gray line: bubble pressure; circles: experimental data).

The major limitation of cubic EoS is that they cannot describe adequately the phase behavior of mixtures of molecules with large size differences and they are unable to accurately calculate liquid densities of the precipitated phase. Accurate modeling of liquid density is essential for an equation of state to predict liquid–liquid equilibrium and their corresponding parameters, such as the solubility parameter, over a range of conditions [69]. Also, the cubic EoS are typically fit to the critical point and asphaltene critical properties are not well defined because asphaltenes decompose before reaching critical points and thus impairing the predictive capabilities for asphaltene onset conditions.

3.3. Robustness of PC-SAFT characterization

The previous results showed that PC-SAFT with the new characterization procedure can represent the system better than the cubic EoS. The robustness of the characterization method is further checked by performing the PC-SAFT parameter estimation as discussed above for a different crude oil (crude C), and with gas injection of 15 mol%. The PC-SAFT predictions and comparison with experimental data points are shown in Fig. 4C. This parameter set was further used to predict the asphaltene phase behavior for other gas injection amounts (Fig. 4A, B and D). The results were impressive as observed from Fig. 4A, B and D due to the good characterization of crude oil with asphaltene as one of its component.

3.4. Sensitivity to SARA

As observed from the characterization procedure, one of the important inputs on which the crude oil is modeled is the SARA. Unfortunately, a disadvantage of the SARA analysis is that fraction measurements by different techniques and/or from different laboratories can show large differences [70,71]. Despite this deficiency SARA analysis is still widely used as a form of characterizing the oil and quantifying the amount of asphaltenes present. An equation of state tuned to an inaccurate SARA is expected to produce inaccurate predictions of phase behavior.

Table 13 shows the SARA reported by two different labs for the same crude C. Because lab 2 in the process of quantifying SARA lost significant amount of light ends in the form of saturates, they reported a higher amount of aromatics and asphaltenes than actually present. To consider the possibility of dealing with an inaccurate SARA data, crude C was fit at 15 mol% of injected gas to an inaccurate SARA. The result is inaccurate predictions of the phase behavior particularly at high injected gas concentration. The conclusion is that, in characterizing a crude oil, care must be taken to fit the equation of state model to accurate data.

3.5. Lower asphaltene onset pressure

Till now we discussed the onset pressures of asphaltene which are above bubble pressure. During the transport of crude oils in a wellbore/pipeline, the pressure depletes and on a pressure–temperature diagram it may follow the path shown with discontinuous black line in Fig. 5. The path followed is a curve because the system is non-isothermal. Point A has high enough pressure such that

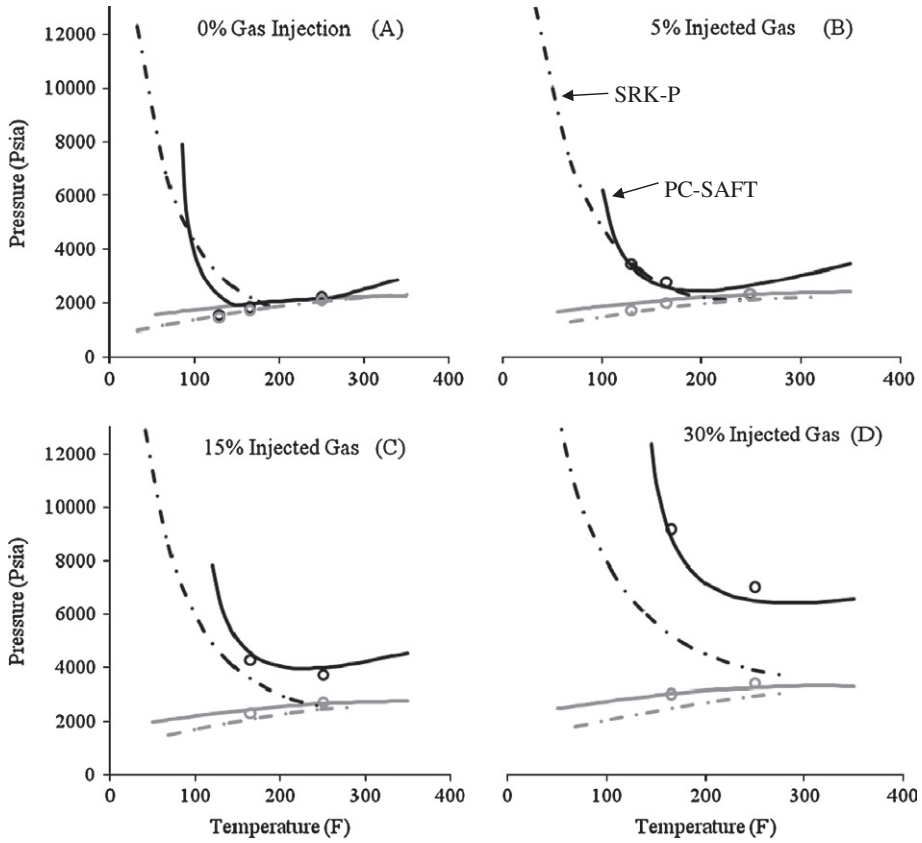

Fig. 3. PC-SAFT and SRK-P characterized oil prediction for crude B after estimating the parameters for 5 mol% of gas injection data (black line: AOP; gray line: bubble pressure; circles: experimental data). Injected gas composition (mol%): N_2-0.4%, CO_2-3.9%, C_1-71.4%, C_2-12%, C_3-7.2%, heavy gas-5.1%.

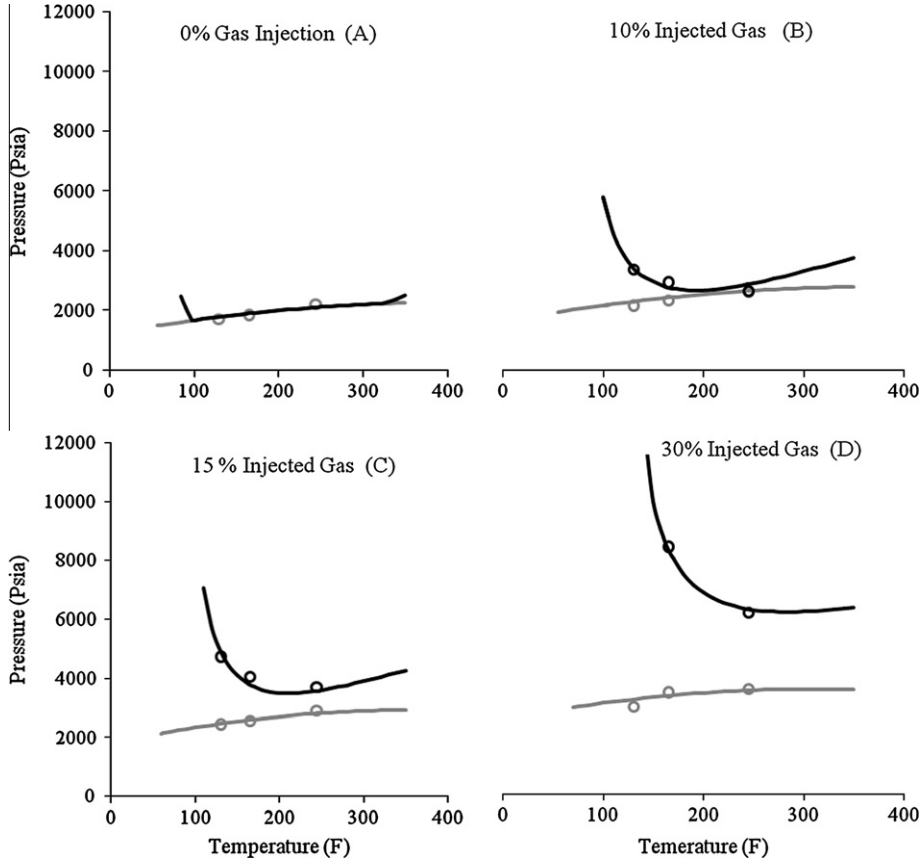

Fig. 4. PC-SAFT characterized oil prediction for crude C after estimating the parameters for the data of 15 mol% of injected gas (black line: AOP; gray line: bubble pressure; circles: experimental data). Injected gas composition (mol%): N_2-0.5%, CO_2-4.5%, C_1-87.4%, C_2-7.2%, C_3-0.4%, heavy gas-0.0%.

Table 13
SARA analysis as reported by two different laboratories for the same crude C.

(wt/wt%)	Saturates	Aromatics + resins	Asphaltenes
Lab 1	73.42	26.37	0.17
Lab 2	49.5	47.4	3.1

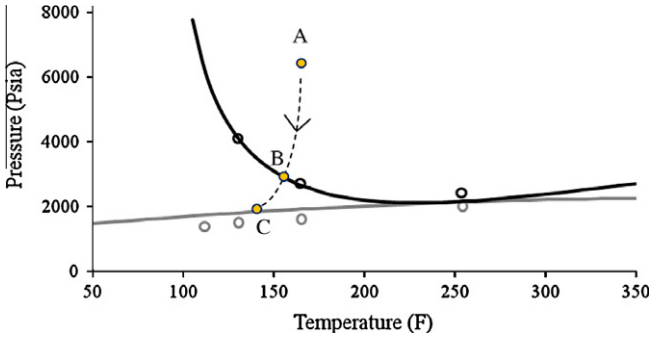

Fig. 5. Path followed by a PT curve of crude oil A from reservoir condition to its bubble pressure in a wellbore during production (black line: AOP; gray line: bubble pressure; discontinuous black line: pressure drop in wellbore).

asphaltenes are stable in oil, Point B lies on asphaltene phase boundary below which asphaltenes precipitate and Point C lies on the bubble pressure curve. The curve from Point A crosses over the asphaltene onset pressure (Point B) and reaches the bubble pressure (Point C). From Point B to Point C liquid–liquid equilibrium exists. This pressure depletion along the length of the wellbore is also schematically shown in Fig. 6A. With further depletion of pressure along the wellbore, the system arrives to its bubble point, where the light components that are asphaltene precipitants, escape from the liquid phase. As this happens, the solubility parameter of the oil increases until the oil becomes a better asphaltene solvent and asphaltene becomes stable in the oil phase again [21]. Thus, once we reach bubble pressure at our original gas content, with further pressure depletion we travel along a pressure–composition curve {as per the experimental procedure of lower AOP [72]} as shown in Fig. 6B for a constant temperature of 120 F. Below a particular gas content (Point D), the asphaltenes become completely soluble in crude oil. This is called the lower asphaltene onset for this temperature.

Wellbore/pipeline systems are not isothermal, thus forcing us to analyze the pressure depletion curve from a two variables point of view (gas content and temperature). This results in a 3D asphaltene phase plot between pressure, temperature and gas content as shown in Fig. 7. Now the pressure depletion curve (for crude oil system in a wellbore) can be followed in the phase plot very easily as represented by the black line in Fig. 7.

As mentioned before, the escape of lighter ends makes crude oil a good solvent for asphaltenes [73] and the trend is seen from the 3D phase plot with decreasing AOP. Also with less light components in the liquid phase, the bubble pressure decreases. In the literature there are studies that also report the lower asphaltene onset pressure curves (conditions below which asphaltenes becomes stable in the oil again), typically plotted on a P–T diagram at constant gas content [74,75]. According to such a representation, it means that for a system at constant overall composition there exists an upper asphaltene onset and a lower asphaltene onset for every temperature. Thus for a range of temperatures, with varying composition we get different lower onsets which when interpolated on the pressure–temperature diagram looks like the green star marker line in Fig. 8.

3.6. Precipitated asphaltene rich phase

Along with crude oil characterization and asphaltene phase behavior, another aspect of interest for the oil industry is the asphaltene deposition profile [76]. Both academics and industries are actively involved in the development of asphaltene deposition simulator [76–79]. For such a program, an essential initial boundary condition is the amount of asphaltene that can precipitate and

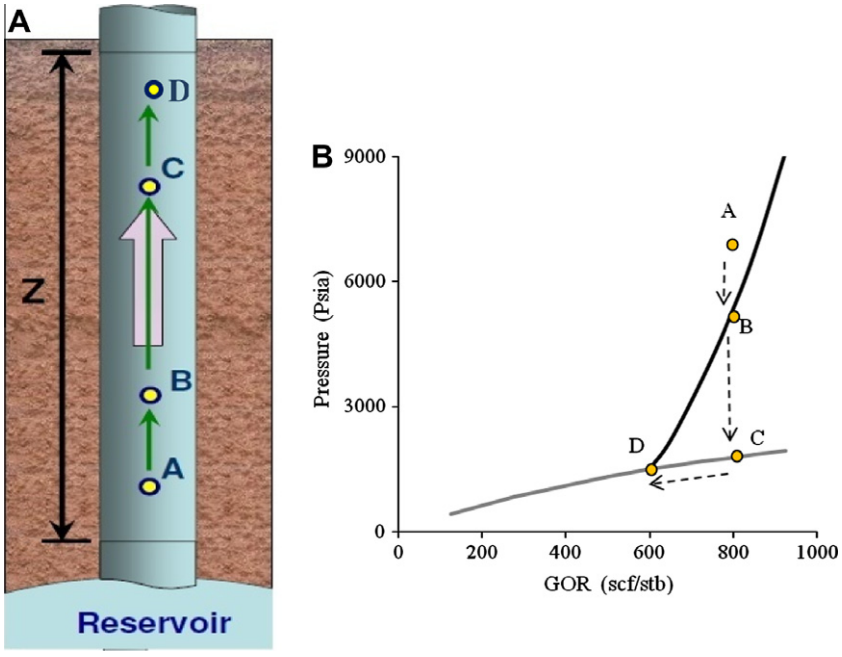

Fig. 6. AOP behavior of crude oil A with respect to gas content in crude oil at a constant temperature of 120 F (black line: AOP; gray line: bubble pressure).

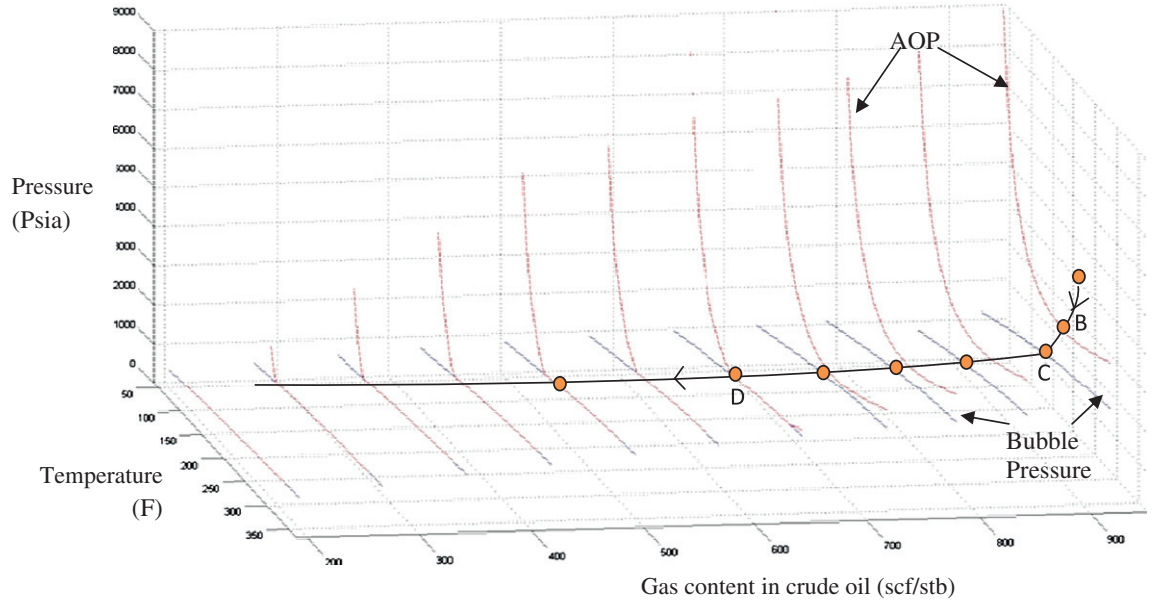

Fig. 7. 3D asphaltene phase plot with the path followed by the PT curve along the length of wellbore for for Crude A (red line: AOP; blue line: bubble pressure; black line: Pressure drop in wellbore). (For interpretation of the references to color in this figure legend, the reader is referred to the web version of this article.)

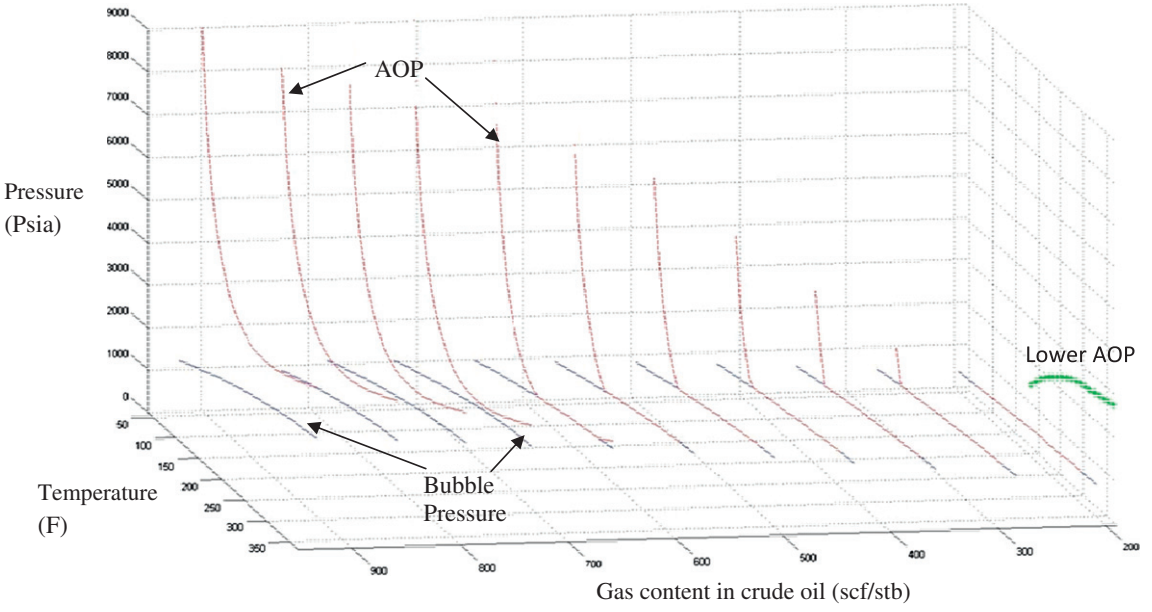

Fig. 8. 3D phase plot along with asphaltene lower onset pressures for crude A (red line: AOP; blue line: bubble pressure; green line: lower AOP). (For interpretation of the references to color in this figure legend, the reader is referred to the web version of this article.)

hence deposit [7]. After characterizing the crude oil with the above mentioned procedure and modeling the asphaltene phase behavior, at any given temperature and pressure one can say whether the oil will split into two liquid fractions of asphaltene rich and lean phases. From the phase diagrams, we observe that maximum driving force and hence maximum amount of asphaltene precipitated at a given temperature is at its bubble point. For a system at bubble pressure, Fig. 9 shows the weight percent of asphaltene precipitated with respect to STO (crude B). Thus the maximum percent that can be precipitated is the asphaltene content reported by SARA.

The results are in accordance with the phase plots as more asphaltene are precipitated with increasing injected gas. Also from the phase plot we observe that at lower temperatures instability of asphaltenes increases. The maximum amount of asphaltenes that can be precipitated is the amount of asphaltenes in crude oil. For 30% of injected gas and above, from Fig. 9 we can observe that almost all the asphaltenes present in oil are precipitated as percent of asphaltene precipitated is ~0.2% while SARA reports ~0.21%. Bulk filtration data at 100 psia above the saturation pressure was available at three different temperatures, without gas injection. Consequent to filtration, filter retained solid asphaltene particles

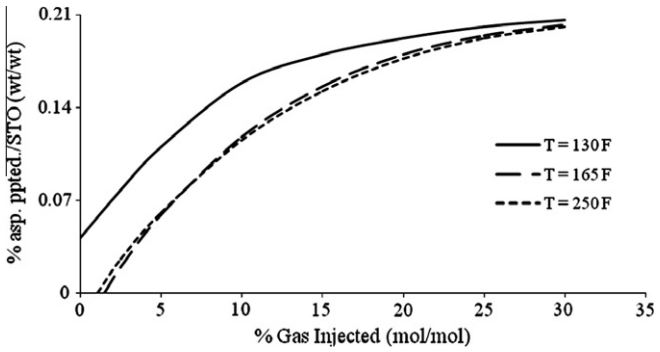

Fig. 9. Crude B asphaltene precipitation curve for different amounts of injected gas at three different temperatures.

Table 14
Amount of asphaltene in precipitated phase of crude A.

Temperature (F)	Mole percentage of asphaltene in precipitated phase	Weight percentage of asphaltene in precipitated phase
130	15.2	72.45
165	11.8	66.91
254	7.9	57.24

larger than 0.22 μm, the smaller asphaltene particles stuck to the wall of the NIR cell, while the unprecipitated asphaltene remained in the filtrate. Thus the data could not be quantified for reproducing the results.

Table 14 shows the estimated amount of asphaltene in the precipitated phase of Crude A at the bubble pressures, and will be helpful in the design of solvent deasphalters. It is interesting to observe the enrichment of asphaltene in the precipitated phase (~10 mol%) from a very lean oil phase of ~0.1 asphaltene mol%.

4. Conclusion

PC-SAFT is a highly promising equation of state for modeling asphaltene precipitation. With this work, we have demonstrated a brief methodology to characterize crude oils using PC-SAFT EoS and subsequently model asphaltene phase behavior in crude oils. This work describes a methodology by which several similar components can be lumped together as one fraction and thus drastically decreasing the computational expense in performing these thermodynamic calculations. PC-SAFT parameters can then be calculated for each of these fractions based on the correlations provided in this work. A systematic methodology to perform the PC-SAFT parameter estimation is also explained in this work which will facilitate easy usage of this EoS to model other crude oils. Phase behavior calculations were performed for different crude oils in the presence of different amounts of injected gas and the results were compared against similar calculations performed with a cubic EoS. It was observed that in case of PC-SAFT, a single set of parameters was sufficient to describe the phase behavior of the oil with various gas injection amounts. However, for a cubic EoS one set of parameters failed to sufficiently describe the experimental observations for other gas injection amounts.

The asphaltene phase behavior curves were plotted on pressure–temperature and pressure–composition axis. These curves were then combined to show the pressure depletion in a well bore on an asphaltene phase envelope and to explain the lower asphaltene onset pressure. Based on the predicted asphaltene phase envelope, the amount of precipitated asphaltene was computed. Such modeling is essential for an asphaltene deposition simulator and solvent deasphalters.

5. Acronyms

PC-SAFT	Perturbed Chain form of the Statistical Associating Fluid Theory
SRK-P	Soave–Redlich–Kwong–Peneloux
SCN	single carbon number
STO	stock tank oil/dead oil
GOR	gas-to-oil ratio
EoS	equation of state
RI	refractive index
A+R	aromatics + resins
SARA	saturates, aromatics, resins and asphaltenes
PNA	poly-nuclear-aromatic
MW	molecular weight
AOP	asphaltene onset pressure
NIR	near infrared

Acknowledgments

This work was undertaken with the funding from ADNOC's Oil R&D Subcommittee. The authors are thankful to Shahin Negahban, Marwan Haggag, Dalia Abdullah, Sanjay Misra and the Enhanced Oil Recovery Technical Committee for valuable support. The authors also thank George Hirasaki, Jefferson Creek, Jianxin Wang, Hariprasad Subramani and Jill Buckley for helpful discussions.

References

[1] Vargas FM, Gonzalez DL, Ceek JL, Wang J, Buckley J, Hirasaki GJ, et al. Development of a general method for modeling asphaltene stability. Energy Fuels 2009;23:1147–54.
[2] Mitchell DL, Speight JG. Solubility of asphaltenes in hydrocarbon solvents. Fuel 1973;52(2):149–52.
[3] Yen TF, Erdman JG, Pollack SS. Investigation of the structure of petroleum asphaltenes by X-ray diffraction. Anal Chem 1961;33(11):1587–94.
[4] Creek JL. Freedom of action in the state of asphaltenes: escape from conventional wisdom. Energy Fuels 2005;19(4):1212–24.
[5] Escobedo J, Mansoori GA. Theory of viscosity as a criterion for determination of onset of asphaltene flocculation. SPE J 1996 [SPE paper 28729].
[6] Grutters M, Huoa Z, Ramanathana K, Naafsa D, Clarkea E, Abdallahc D, et al. Using geochemistry to identify and control asphaltene deposition and improve flow assurance strategies in onshore middle-east carbonate fields. In: Petrophase conference 2010, Jersey City; June 13–17, 2010.
[7] Vargas FM, Ceek JL, Chapman WC. On the development of an asphaltene deposition simulator. Energy Fuels 2010;24(4):2294–9.
[8] Katz DL, Firoozabadi A. Predicting phase behavior of condensate/crude-oil systems using methane interaction coefficients. J Petrol Technol 1978;30(11):1649–55.
[9] Roenningsen HP, Skjevrak I, Osjord E. Characterization of North Sea petroleum fractions: hydrocarbon group types, density and molecular weight. Energy Fuels 1989;3(6):744–55.
[10] Whitson CH. Characterizing hydrocarbon plus fractions. SPE J 1983;23(4):683–94 [SPE Paper 12233].
[11] Riazi MR, Daubert TE. Simplify property predictions. Hydrocarbon Process 1980;60(3):115–6.
[12] Tarek A. Hydrocarbon phase behavior. 1st ed. Houston: Gulf Publishing Company; 1989.
[13] Riazi MR, Taher A. Physical properties of heavy petroleum fractions and crude oils. Fluid Phase Equilib 1996;117(1–2):217–24.
[14] Riazi MR. A continues model for C7+ fraction characterization of petroleum fluids. Ind Eng Chem Res 1997;36(10):4299–307.
[15] Leelavanichkul P, Deo MD, Hanson FV. Crude oil characterization and regular solution approach to thermodynamic modeling of solid precipitation at low pressure. Pet Sci Technol 2004;22(7–8):973–90.
[16] Buckley J, Hirasaki GJ, Liu Y, Von Drasek S, Jianxin W, Gill BS. Asphaltene precipitation and solvent properties of crude oils. Pet Sci Technol 1998;16(3–4):251–85.
[17] GC, Mansoori AG. Advances in thermodynamics : C7+ fraction characterization, vol. 1. Portland: Taylor & Francis; 1989.
[18] Chapman WG, Gubbins KE, Jackson G, Radosz M. SAFT: equation-of-state solution model for associating fluids. Fluid Phase Equilib 1989;52:31–8.
[19] Chapman WG, Gubbins KE, Jackson G, Radosz M. New reference equation of state for associating liquids. Ind Eng Chem Res 1990;29(8):1709–21.
[20] Pedersen KS, Christensen PL. Phase behavior of petroleum reservoir fluids. 1st ed. Boca Raton: CRC Press; 2007.

[21] Ting PD, Hirasaki GJ, Chapman WG. Modeling of asphaltene phase behavior with the SAFT equation of state. Pet Sci Technol 2003;21(3–4):647–61.
[22] Gross J, Sadowski G. Perturbed-chain SAFT: an equation of state based on a perturbation theory for chain molecules. Ind Eng Chem Res 2001;40(4):1244–60.
[23] Dominik A, Chapman WG. Thermodynamic model for branched polyolefins using the PC-SAFT equation of state. Macromolecules 2005;38(26):10836–43.
[24] Rao BKB. Modern petroleum refining. 4th ed. Delhi: Oxford-IBH; 2005.
[25] Gonzalez DL, Ting PD, Hirasaki GJ, Chapman WG. Prediction of asphaltene instability under gas injection with the PC-SAFT equation of state. Energy Fuels 2005;19(4):1230–4.
[26] Gonzalez DL, Hirasaki GJ, Chapman WG. Modeling of asphaltene precipitation due to changes in composition using the perturbed chain statistical associating fluid theory equation of state. Energy Fuels 2007;21(3):1231–42.
[27] Mullins OC. The modified Yen model. Energy Fuels 2010;24(4):2179–207.
[28] Spiecker PM, Keith LG, Kilpatrick PK. Aggregation and solubility behavior of asphaltenes and their subfractions. J Colloid Interf Sci 2003;267(1):178–93.
[29] Zao JY, Mullins OC, Chengli D, Dan Z. Modeling of asphaltene grading in oil reservoirs. Nat Resour 2010;1(1):19–27.
[30] Buckley JS. Predicting the onset of asphaltene precipitation from refractive index measurements. Energy Fuels 1999;13(2):328–32.
[31] Ting PD. Thermodynamic stability and phase behavior of asphaltenes in oil and of other highly asymmetric mixtures. PhD Thesis, USA: Rice University; 2003.
[32] Gonzalez DL, Vargas FM, George JH, Chapman WG. Modeling study of CO_2-induced asphaltene precipitation. Energy Fuels 2008;22(2):757–62.
[33] Brown TS, Niesen NV, Sloan ED, Kidnay AJ. Vapor–liquid equilibria for the binary systems of nitrogen, carbon dioxide, and *n*-butane at temperatures from 220 to 344 K. Fluid Phase Equilib 1989;53:7–14.
[34] Besserer GJ, Robinson DB. Equilibrium-phase properties of nitrogen–hydrogen sulfide system. J Chem Eng Data 1975;20(2):157–61.
[35] Stryjek R, Chappelear PS, Kobayashi R. Low-temperature vapor–liquid equilibria of nitrogen–methane system. J Chem Eng Data 1974;19(4):334–9.
[36] Stryjek R, Chappelear PS, Kobayashi R. Low-temperature vapor–liquid equilibria of nitrogen–ethane system. J Chem Eng Data 1974;19(4):340–3.
[37] Kalra H, Robinson DB, Besserer GJ. The equilibrium phase properties of the nitrogen-*n*-pentane system. J Chem Eng Data 1977;22(2):215–8.
[38] Cordova TG, García DNJ, Flores BEG, Sanchez FG. Vapor–liquid equilibrium data for the nitrogen dodecane system at temperatures from (344 to 593) K and at pressures up to 60 MPa. J Chem Eng Data 2011;56(4):1555–64.
[39] Richon D, Laugler S, Renon H. High-pressure vapor-liquid equilibrium data for binary mixtures containing N_2, CO_2, H_2S, and an aromatic hydrocarbon or propylcyclohexane in the range 313–473 K. J Chem Eng Data 1992;37(2):264–8.
[40] Bierlei JA, Kay WB. Phase-equilibrium properties of system carbon dioxide-hydrogen sulfide. Ind Eng Chem 1953;45(3):618–24.
[41] Bian B, Wang Y, Shi J. Simultaneous determination of vapor–liquid equilibrium and molar volumes for coexisting phases up to the critical temperature with a static method. Fluid Phase Equilib 1993;90(1):177–87.
[42] Ohgaki K, Katayama T. Isothermal vapor–liquid equilibrium data for the ethane–carbon dioxide system at high pressures. Fluid Phase Equilib 1977;1(1):27–32.
[43] Kim JH, Kim MS. Vapor–liquid equilibria for the carbon dioxide + propane system over a temperature range from 253.15 to 323.15 K. Fluid Phase Equilib 2005;238(1):13–9.
[44] Besserer GJ, Robinson DB. Equilibrium-phase properties of *n*-pentane–carbon dioxide system. J Chem Eng Data 1973;18(4):416–9.
[45] Camacho LEC, Luna LAG, Solis OE, Ramirez ZM. New isothermal vapor–liquid equilibria for the CO_2 + *n*-nonane, and CO_2 + *n*-undecane systems. Fluid Phase Equilib 2007;259(1):45–50.
[46] Morris WO, Donohue MD. Vapor–liquid equilibria in mixtures containing carbon dioxide, toluene, and 1-methylnaphthalen. J Chem Eng Data 1985;30(3):259–63.
[47] Kohn JP, Kurata F. Heterogeneous phase equilibria of the methane–hydrogen sulfide system. AIChE J 1958;4(2):211–7.
[48] Kay WB, Brice DB. Liquid–vapor equilibrium relations in ethane–hydrogen sulfide system. Ind Eng Chem 1953;45(3):615–8.
[49] Gilliland ER, Scheeline HW. High-pressure vapor–liquid equilibrium for the systems propylene–isobutane and propane–hydrogen sulfide. Ind Eng Chem 1940;32(1):48–54.
[50] Reamer HH, Sage BH, Lacey WN. Phase equilibria in hydrocarbon systems volumetric and phase behavior of *n*-pentane–hydrogen sulfide system. Ind Eng Chem 1953;45(8):1805–9.
[51] Yokoyama C, Usui A, Takahashi S. Solubility of hydrogen sulfide in isooctane, *n*-decane, *n*-tridecane, *n*-hexadecane and squalane at temperatures from 323 to 523 K and pressures up to 1.6 MPa. Fluid Phase Equilib 1993;85:257–69.
[52] Laugier S, Richon D. Vapor-liquid equilibria for hydrogen sulfide + hexane, + cyclohexane, + benzene, + pentadecane, and + (hexane + pentadecane). J Chem Eng Data 1995;40(1):153–9.
[53] Wichterle I, Kobayashi R. Vapor–liquid equilibrium of methane–ethane system at low temperatures and high pressures. J Chem Eng Data 1972;17(1):9–12.
[54] Wichterle I, Kobayashi R. Vapor–liquid equilibrium of methane–propane system at low temperatures and high pressures. J Chem Eng Data 1972;17(1):4–9.
[55] Chu TC, Chen RJJ, Chappelear PS, Kobayashi R. Vapor–liquid equilibrium of methane-*n*-pentane system at low temperatures and high pressures. J Chem Eng Data 1976;21(1):41–4.
[56] Srivastan S, Darwish NA, Gasem KAM, Rabinson RL. Solubility of methane in hexane, decane, and dodecane at temperatures from 311 to 423 K and pressures to 10.4 MPa. J Chem Eng Data 1992;37(4):516–20.
[57] Lin HM, Sebastian HM, Simnick JJ, Chao KC. Gas–liquid equilibrium in binary mixtures of methane with *n*-decane, benzene, and toluene. J Chem Eng Data 1979;24(2):146–9.
[58] Matscike DE, Thodos GT. Vapor–liquid equilibria for the ethane–propane system. J Chem Eng Data 1962;7(2):232–4.
[59] Bufkin BA, Rabinson RL, Esirera SS, Luks KD. Solubility of ethane in *n*-decane at pressures to 8.2 MPa and temperatures from 278 to 411 K. J Chem Eng Data 1986;31(4):421–3.
[60] Ohgaki K, Sano F, Katayama T. Isothermal vapor–liquid equilibrium data for binary systems containing ethane at high pressures. J Chem Eng Data 1976;21(1):55–8.
[61] Oxley JA. Phase relations of binary hydrocarbon systems propane-*n*-pentane. MS thesis, USA: The Ohio State University; 1962.
[62] Richon D, Laugler S, Renon H. High-pressure vapor–liquid equilibria for binary mixtures containing a light paraffin and an aromatic compound or a naphthene in the range 313–473 K. J Chem Eng Data 1991;36(1):104–11.
[63] Rice P, Nikheli AE. Isothermal vapour–liquid equilibrium data for the systems *n*-pentane with *n*-hexane, *n*-octane and *n*-decane. Fluid Phase Equilib 1995;107(2):257–67.
[64] Wang JLH, Lu BCY. Vapour–liquid equilibrium data for the *n*-pentane–benzene system. J Appl Chem Biotechnol 1971;21(10):297–9.
[65] Gonzalez DL. Modeling of asphaltene precipitation and deposition tendency using the PC-SAFT equation of state. PhD Thesis, USA: Rice University; 2008.
[66] Jog PK, Chapman WG, Gupta SK, Swindoll RD. Modeling of liquid–liquid-phase separation in linear low-density polyethylene-solvent systems using the statistical associating fluid theory equation of state. Ind Eng Chem Res 2002;41(5):887–91.
[67] Dudášová D, Silset A, Sjöblom J. Quartz crystal microbalance monitoring of asphaltene adsorption/deposition. J Dispersion Sci Technol 2008;29(1):139–46.
[68] Modaresghazani J, Satyro MA, Yarranton HW. Conventional cubic equation of state modeling of the phase behavior of bitumen and solvents. In: Petrophase conference 2010, Jersey City; June 13–17, 2010.
[69] Vargas FM, Panuganti S, Gonzalez DL, Chapman WG. Advances in predicting asphaltene precipitation at high pressure and temperature. Managing scale & asphaltene SPE ATW 2010, Abu Dhabi; November 28–December 1, 2010.
[70] Fan T, Buckley JS. Rapid and accurate SARA analysis of medium gravity crude oils. Energy Fuels 2002;16(6):1571–5.
[71] Kharrat AM, Zacharia J, Cherian VJ, Anyatonwu A. Issues with comparing SARA methodologies. Energy Fuels 2007;21(6):3618–21.
[72] Hammami A, Phelps CH, Monger-McClure T, Little TM. Asphaltene precipitation from live oils: an experimental investigation of onset conditions and reversibility. Energy Fuels 2000;14(1):14–8.
[73] Vargas FM, Gonzalez DL, Hirasaki GJ, Chapman WG. Modeling asphaltene phase behavior in crude oil systems using the perturbed chain form of the statistical associating fluid theory (PC-SAFT) equation of state. Energy Fuels 2009;23(3):1140–6.
[74] Zhidong L, Firoozabadi A. Cubic-plus-association equation of state for asphaltene precipitation in live oils. Energy Fuels 2010;24(5):2956–63.
[75] Akbarzadeh K, Hammami A, Kharrat A, Zhan D, Allenso S, Creek JL, et al. Asphaltenes—problematic but rich in potential. Oilfield Rev 2007;19(2):22–43.
[76] Akbarzadeh K, Ratulowski J, Lindvig T, Davis T, Huo Z, Broze G. The importance of asphaltene deposition measurements in the design and operation of subsea pipelines. In: SPE annual technical conference and exhibition 2009, New Orleans; October 4–7, 2009 [SPE paper 124956].
[77] Ramirez-Jaramillo E, Lira-Galeana C, Manero O. Modeling asphaltene deposition in production pipelines. Energy Fuels 2006;20(3):1184–96.
[78] Soltani SB, Rashtchian D, Tohidi B, Jamialahmadi M. Integrated modeling methods for asphaltene deposition in wellstring. J Jpn Pet Inst 2009;52:322–31.
[79] Vargas FM, Creek JL, Chapman WG. Development of an asphaltene deposition simulator. In: Petrophase conference 2009, Rio de Janeiro; June 14–18, 2009.